JTTEE5 4:408-414

Heat Transfer Between WC-Co Coating and Aluminum Alloy Substrate During High-Velocity Oxygen-Fuel (HVOF) Spraying

V.V. Sobolev, J.M. Guilemany, J.A. Calero, and F.J. Villuendas

Mathematical simulation of the heat transfer between a WC-Co coating and an aluminum alloy (Al-4%Cu) substrate during HVOF spraying is provided. This simulation includes the investigation of temperature evolution, coating solidification, fusion and solidification in the substrate interfacial region, and particular features of the substrate-coating thermal interaction. Optimal thermal conditions for forming the coating structure are estimated. The results obtained are used in another paper (Ref 15), "Formation of Structure of WC-Co Coating on Aluminum Alloy Substrate During High-Velocity Oxygen-Fuel (HVOF) Spraying," to predict the structural parameters, which agree well with the experimental data.

1. Introduction

COATING solidification plays an important role in determining coating structure performance (Ref 1, 2). Solidification behavior depends significantly on the substrate-coating heat transfer during coating deposition. The substrate-coating interfacial region, including the substrate interfacial zone and the first coating layer, is important because in this region adhesive bonds between the thermal spray coating and the substrate are developed (Ref 1-5).

An effective tool for the better understanding and improvement of HVOF spraying technology is a realistic mathematical model of the substrate-coating thermal interaction. Such a model was developed and used in Ref 3 and 7 to predict the formation of WC-Co and WC-Ni coatings on a steel substrate. It gives the results, which agree well with the experimental data (Ref 4, 7).

This model is part of a general model of HVOF spraying, which predicts powder particle in-flight behavior as well as coating deposition and structure formation (Ref 8-12). Similar models for plasma spraying were developed in Ref 13 and 14.

In this paper, the model is applied to WC-Co powder particles sprayed on to the face of a cylinder made of aluminum base alloy (Al-4%Cu). The HVOF system installed in the Centre of Thermal Spraying in the University of Barcelona (Plasma Technik 100) was used. A platform with the cylinders was rotated with a speed of 0.5 ms^{-1} and a time interval of 1.32 s between the application of the subsequent coating layers.

The results of this paper are used in Ref 15 for the modeling of coating structure formation during HVOF spraying of the WC-Co powder on to the Al-4%Cu substrate. The results agree well with the experimental data (Ref 15).

Keywords coating, heat flow, HVOF processing, solidification modeling, substrate

V.V. Sobolev, J.M. Guilemany, J.A. Calero, and **F.J. Villuendas,** Metalurgia Física-Ciencia de Materiales, Departamento de Ingeniería Química y Metalurgia, Universidad de Barcelona, Martí y Franqués, 1, 08028, Barcelona. Spain.

2. Mathematical Model

The model is described in detail in Ref 3. Initially a powder particle agglomerate consists of small carbide WC particles surrounded by the Co-40%W alloy. During particle flight, dissolution of the WC takes place. The particles impinging on to the substrate surface contain mainly carbides of diminished size in the metal matrix alloy Co-W-C (Ref 5).

For this analysis, the impinging mixture of tungsten carbides and the liquid alloy are considered quasi-homogeneous since the carbide sizes (1 to 2 μm) are markedly smaller than the coating layer thickness (~15 μm).

The heat transfer model uses two heat conductivity equations for the substrate temperature, T_1, coating layer temperature, T_2, and associated boundary and initial conditions (Ref 3).

Special attention is paid to the thermal interaction between the first coating layer and the substrate. This interaction is very important from the thermal point of view because it constitutes the main part of the substrate-coating interaction and essentially contributes to the coating-substrate adhesion and bonding.

On the basis of the calculated temperature fields T_1 and T_2, the criteria I_{11}, I_{12}, I_{21}, and I_{22} of the thermal state of the solidifying substances are calculated. They can serve as the indirect criteria of the structure quality for both the first coating layer and subsequent layers and for the substrate interfacial region (Ref 3, 6, 16).

The I_{11} and I_{12} parameters give the mean values of thermal gradients arising during solidification in the substrate interfacial region, and particularly in the first coating layer, which is responsible for the formation of thermal stresses (Ref 3). These gradients are specifically calculated for the first layer because in this layer they are higher than in the subsequent coating layers. The criteria I_{21} and I_{22} determine the mean values of the solidifying substance residence time in the liquid-solid phase (mushy) zone in the substrate interfacial region and in the coating layer, respectively. These values influence the formation of structural defects (porosity, nonmetallic inclusion, etc.) (Ref 3).

When I_{21} and I_{22} are minimized, solidification is optimized and minimizes stresses and structural defects in the coating and in the substrate interfacial region (Ref 3, 6).

The coating material properties are from Ref 3, and those of the substrate aluminum alloy are from Ref 17 and 18. For the basic calculations, the parameters are shown in Table 1.

3. Results and Discussion

3.1 *Coating First Layer*

This layer is formed by the liquid droplets impinging on to the substrate surface. Their heat is removed mainly by transfer into the substrate. The heat exchange between the layer upper surface and the surrounding gas medium in this case is negligible.

Calculation results show that the full solidification time, τ_{sol}, of the first coating layer increases with the layer thickness, δ, and exhibits nonuniform behavior with respect to the layer initial temperature T_{20} (Fig. 1). The nonuniformity is due to the competition between two factors. On the one hand, the growth of T_{20} enhances the layer heat content, and this slows down the solidification process. On the other hand, the increase of T_{20} steepens the transverse thermal gradients, which are the driving forces for the heat removal. Therefore, heat removal increases. This factor is more important for relatively small δ. Thus, the τ_{sol} parameter at first diminishes with T_{20}, attaining its minimal value at $T_{20} \approx 1495$ °C, and then grows. The solidification time, τ_{sol}, increases with the substrate initial temperature, T_{10}.

Some details of the solidification kinetics of the first layer are shown in Table 2. At the moments t_{L1} and t_{S1}, the isotherms of the liquidus and solidus, respectively, appear at the substrate-coating interface. They move toward the layer upper surface and disappear when $t = t_{L2}$ (liquidus) and $t = t_{S2}$ (solidus). The latter is the time of the layer full solidification, τ_{sol}.

The time, $t_{L1} = 0.03$ μs, does not vary with T_{10}, T_{20}, and δ.Time t_{S1}, which is very near t_{L1}, behaves similarly. The t_{L2} time increases with T_{10} and δ, and diminishes with T_{20}. The t_{S2} time exhibits the same behavior with respect to T_{10} and δ, and grows with T_{20}.

The parameter, $\tau_1 = (t_{L2} - t_{L1})t_{S2}^{-1}$, defines the time of existence of the liquidus isotherm. It decreases when T_{20} grows and when δ diminishes, and varies weakly with T_{10}. Table 2 shows that the liquid phase remains in the first layer during 60 to 80% of the full solidification time, t_{S2}, of the layer. The parameter, $\tau_2 = (t_{S2} - t_{L2})t_{S2}^{-1}$, determines the relative time of existence of the solid-liquid (mushy) zone state. This value increases with T_{20}, decreases with δ, and does not vary much with T_{10}. The mushy zone state remains in the coating first layer during 20 to

Table 1 Numerical values of parameters

Substrate thickness	3 mm
Coating layer thickness, δ	15 μm
Substrate initial temperature, T_{10}	20 °C
Heat transfer coefficient at the upper surface of a coating layer, α	1000 $Wm^{-2}K^{-1}$
Contact heat transfer coefficient at the substrate-coating interface, α_{c1}	4×10^6 $Wm^{-2}K^{-1}$
Contact heat transfer coefficient at the layer-layer interface, α_{c2}	1.3×10^6 $Wm^{-2}K^{-1}$
Fluid temperature near a coating layer upper surface, T_b	500 °C
Tungsten volume fraction in a metallic matrix alloy	0.52
Metallic phase volume fraction	0.68

Table 2 Variation of characteristic times of solidification in coating first layer with respect to spraying parameters

T_{10}, °C	T_{20}, °C	δ, μm	t_{L2}, μs	t_{S2}, μs	τ_1	τ_2
20	1482	15	2.47	3.27	0.746	0.245
300	1482	15	2.77	3.67	0.747	0.245
20	1530	15	2.24	3.61	0.612	0.380
20	1482	25	6.81	8.29	0.818	0.179

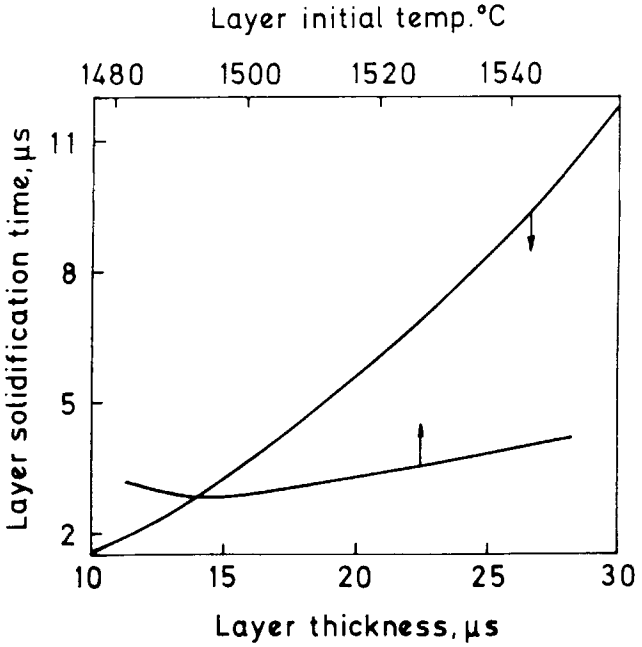

Fig. 1 Variation of layer full solidification time with respect to its thickness and initial temperature

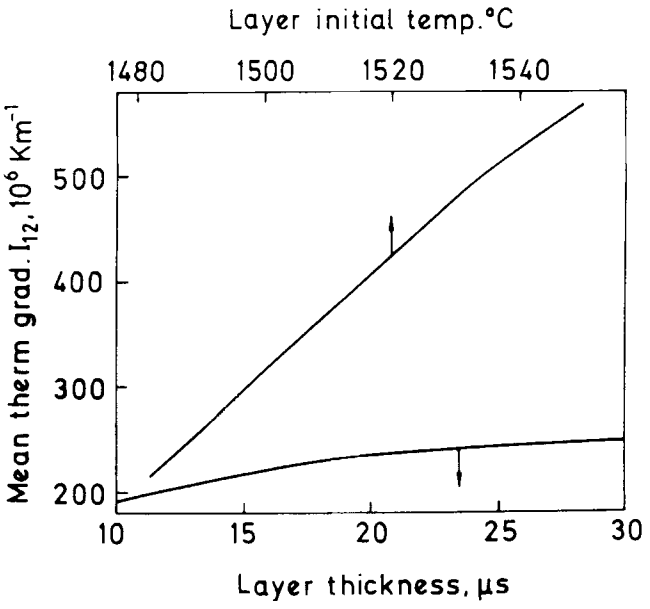

Fig. 2 Variations of mean thermal gradient, I_{12}, with respect to layer thickness and initial temperature

40% of the full solidification time of the layer. The τ_2 parameter grows with T_{20}.

From the behavior of τ_1 and τ_2, in the case of the aluminum alloy substrate, the coating first layer remains in a liquid or mushy zone state during much of its solidification time. These results differ from those obtained when the same WC-Co or WC-Ni coating was formed on a steel substrate (Ref 3, 6). For example, in the latter case (WC-Ni coating), the liquid phase and the mushy zone state remain in the coating first layer during 20 to 30% and 70 to 80%, respectively, of its full solidification time. The percentages with respect to τ_1 and τ_2 in the case of the aluminum alloy substrate are almost reversed.

From Fig. 2, the mean thermal gradient, I_{12}, in the solid phase growing during the solidification of the layer increases with layer thickness, δ, and initial temperature, T_{20}, as both of these factors enhance layer heat content.

Increasing the substrate initial temperature, T_{10}, decreases heat removal from the coating layer, diminishes the thickness of the solidifying solid phase, and smoothes its temperature distribution. The competition between these factors causes the nonuniform behavior of I_{12} with respect to T_{10} (Fig. 3).

As mentioned, the minimal values of I_{12} correspond to the minimal thermal stresses developed in the first coating layer during thermal spraying. Note that the probability of stress formation here is higher than in the subsequent layers. From Fig. 2 and 3, when $\delta = 15$ μm, the minimal thermal stresses are likely to occur if $T_{10} = 200$ °C and $T_{20} = 1497$ °C. The maximum stresses seem to arise when $T_{10} = 300$ °C. Thus, the substrate initial temperature, T_{10}, is a critical parameter for the development of thermal stresses.

Figures 3 and 4 show that the mean value of the solidifying alloy residence time in the mushy zone, I_{22}, varies nonuniformly with respect to δ, T_{10}, and T_{20}. The optimal layer structure formed during its solidification corresponds to the minimal values of I_{22}, and it is possible to predict that this structure can arise under the following process parameters: $\delta = 10$ to 15 μm, $T_{10} = 20$ °C, and $T_{20} = 1510$ °C. A significant change in the structure is expected when $\delta = 20$ μm, $T_{10} = 300$ °C, and $T_{20} = 1550$ °C.

Sometimes different conditions must be fulfilled to obtain minimal values of I_{12} and I_{22} in the same process (Ref 16). The significance of the different coating structural defects in each particular case must be estimated to select the most critical defects (for example, thermal stresses) and to minimize them. In our case, such conditions for minimal stress correspond approximately to $\delta = 10$ to 15 μm, $T_{10} = 200$ °C, and $T_{20} = 1500$ °C.

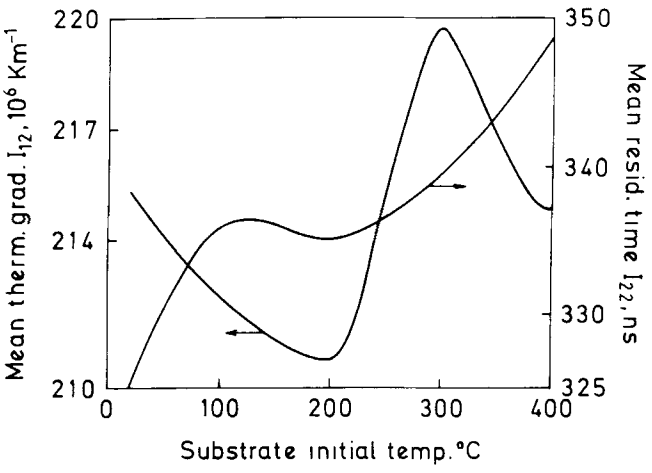

Fig. 3 Variations of mean thermal gradient, I_{12}, and mean residence time, I_{22}, with respect to substrate initial temperature

3.2 *Substrate Interfacial Region*

Due to heat transfer from the coating layer, the substrate interfacial region undergoes melting and subsequent solidification. The times for these processes are presented in Table 3.

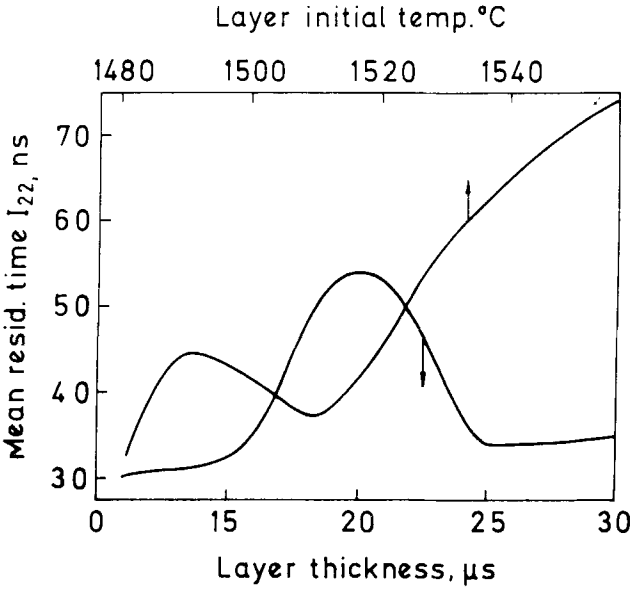

Fig. 4 Variation of mean residence time, I_{22}, with respect to layer thickness and initial temperature

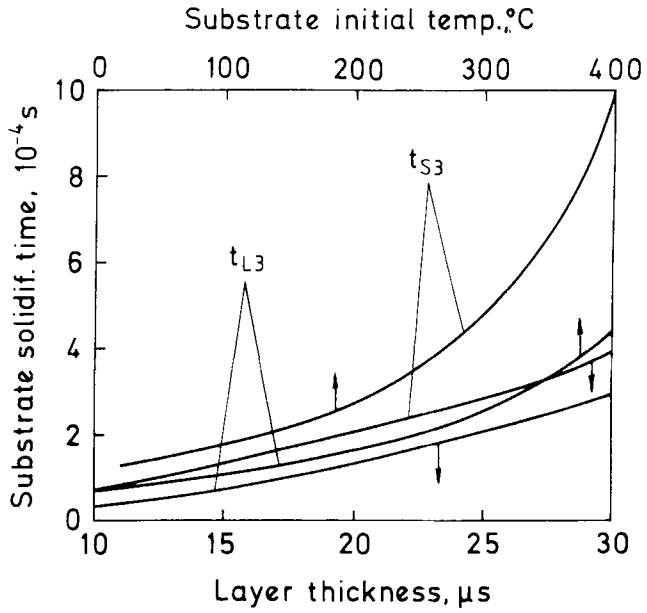

Fig. 5 Variation of substrate solidification times with respect to layer thickness and substrate initial temperature

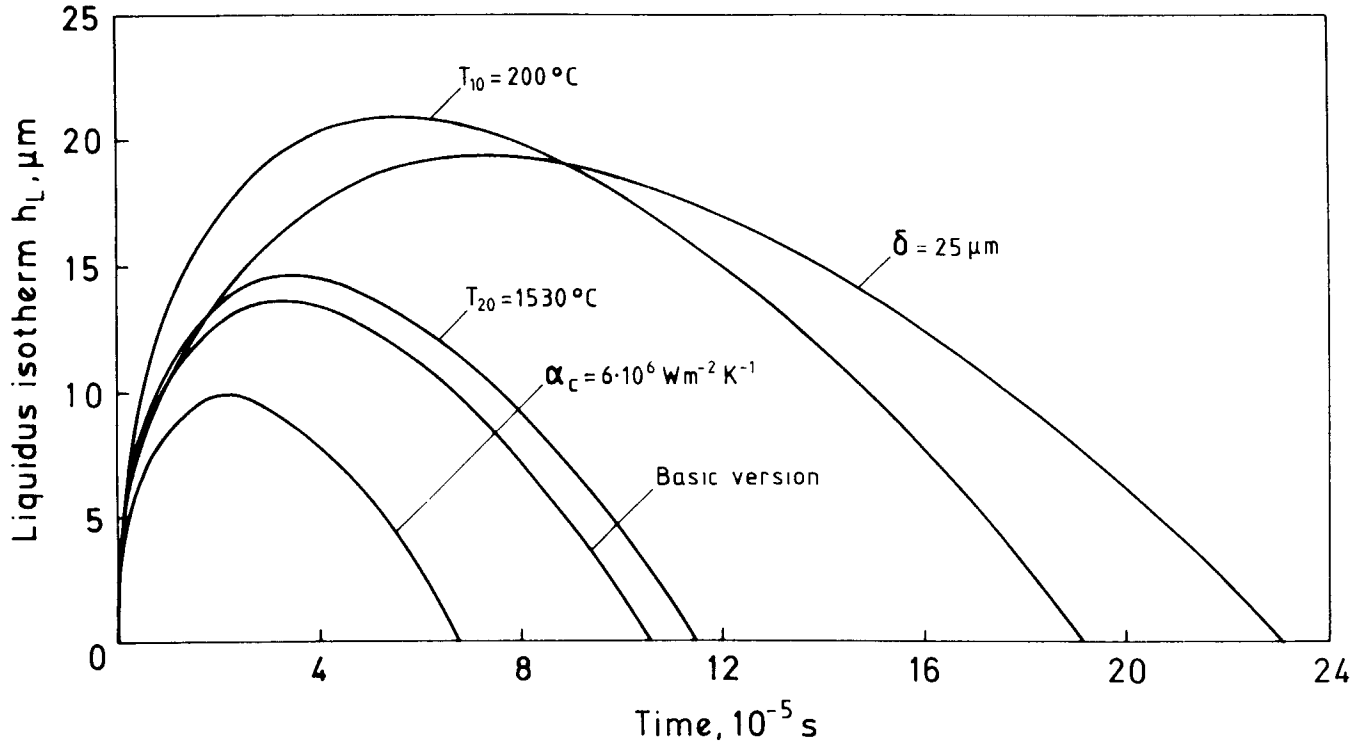

Fig. 6 Variation of position of liquidus isotherm in substrate with respect to time

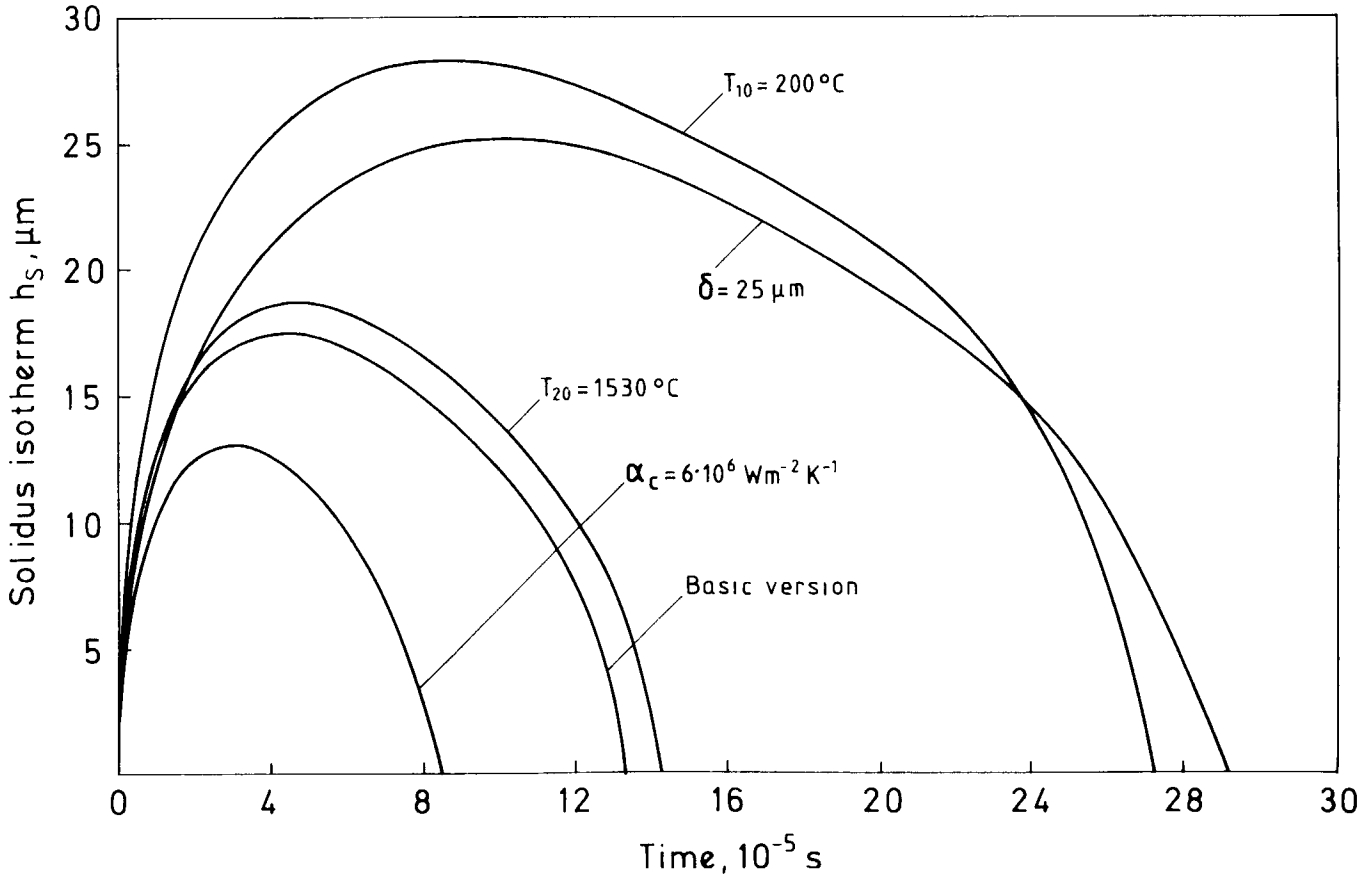

Fig. 7 Variation of position of solidus isotherm in substrate with respect to time

Melting starts when the solidus isotherm $T = T_{S1}$ appears at the substrate-coating interface at the moment $t = t_{S1} = 0.31$ μm. It moves into the substrate with a parameter, h_S (equal to the distance between the interface and the position of the solidus isotherm), determining its displacement with respect to the interface. Displacement is maximal when h_S has the maximal value h_{Sm} defining the substrate melting depth.

The liquidus isotherm appears at the interface at $t = t_{L1}$, which is very near t_{S1}, and moves into the substrate. Parameter h_L gives its displacement with respect to the interface. Its maximal value, h_{Lm}, is the upper limit of the solid-liquid zone in the substrate interfacial region.

After melting is completed, solidification starts. At first, the liquidus isotherm begins to move toward the interface at $t = t_{L2}$, reaching it at $t = t_{L3}$. Later, at $t = t_{S2}$, solidus isotherm movement starts, and this isotherm comes to the interface at $t = t_{S3}$. The parameters $\tau_3 = (t_{L3} - t_{L2})t_{S3}^{-1}$ and $\tau_4 = (t_{S3} - t_{S2})t_{S3}^{-1}$ are the relative times of movement of the liquidus and solidus isotherms, respectively.

From Table 3, t_{L2}, t_{S2}, t_{L3}, and t_{S3} increase with δ, T_{10}, and T_{20}. The τ_3 parameter diminishes as T_{10} grows and T_{20} decreases, and does not vary much with δ. The increase of T_{10} and T_{20} gives rise to τ_4. This parameter decreases with δ. The substrate interfacial region remains in the mushy state during a significant portion of its solidification time.

Table 3 Variation of characteristic times of solidification of substrate interfacial region with respect to spraying parameters

T_{10}, °C	T_{20}, °C	δ, μm	t_{L2}, μs	t_{S2}, μs	t_{L3}, μs	t_{S3}, μs	τ_3	τ_4
20	1482	15	33.0	43.4	106 6	135.3	0.544	0.679
300	1482	15	78.2	142.1	287.5	469.9	0.444	0.700
20	1530	15	35.1	46.5	114.9	145.8	0.547	0.681
20	1482	25	73.7	98.3	232.0	290.9	0.544	0.662

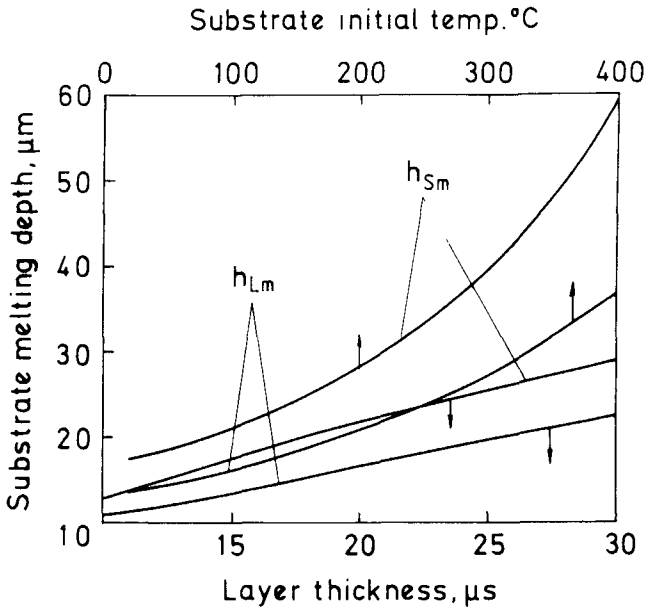

Fig. 8 Variation of susbtrate melting depth with respect to layer thickness and substrate initial temperature

The values of t_{L3} and t_{S3} increase with the layer thickness, δ, and substrate initial temperature, T_{10} (Fig. 5). The difference between t_{L3} and t_{S3} rises with T_{10} and weakly varies with δ. These times also grow when the layer initial temperature, T_{20}, increases.

The general view of the liquidus and solidus isotherms corresponding to their maximal penetration into the substrate interfacial region during melting is shown in Fig. 6 and 7. Their zones of penetration widen with increasing δ, T_{10}, and T_{20} and narrow with increasing α_c. The maximum values of h_{Lm} and h_{Sm} increase when the parameters δ, T_{10}, and T_{20} grow (Fig. 8). The difference between h_{Lm} and h_{Sm}, which determines the extent of the mushy zone region, increases with T_{10} and weakly varies with δ.

An understanding of the formation of the substrate structure in its interfacial region during solidification requires knowledge of the variation of the mean thermal gradient, I_{11}, in the solidifying solid phase and the mean residence time, I_{21}. The I_{11} parameter diminishes with increasing δ and T_{10} (Fig. 9). It exhibits nonuniform behavior with respect to T_{20}, having a minimal value at $T_{20} = 1510$ °C. The criterion, I_{21}, grows with T_{20} and behaves nonuniformly when δ and T_{10} increase. It has minimal values at δ = 15 to 22 μm and $T_{10} = 200$ °C. Thus, thermal stresses are expected to be minimized when $T_{20} \approx 1510$ °C, and the optimal structure in the substrate interfacial region seems to develop if δ = 15 to 22 μm and $T_{10} = 200$ °C.

3.3 *Subsequent Coating Layers*

The influence of the subsequent coating layers on heat transfer, particularly in the substrate-coating interfacial region, essentially depends on the thermophysical properties of the substrate and coating materials. References 3 and 5 show that, for the HVOF sprayed WC-Co coating on a steel substrate, the influence of the second layer is very weak and that of subsequent layers decreases, nearly vanishing with the fourth layer. Thus, in that case, the interfacial heat transfer is determined mainly by

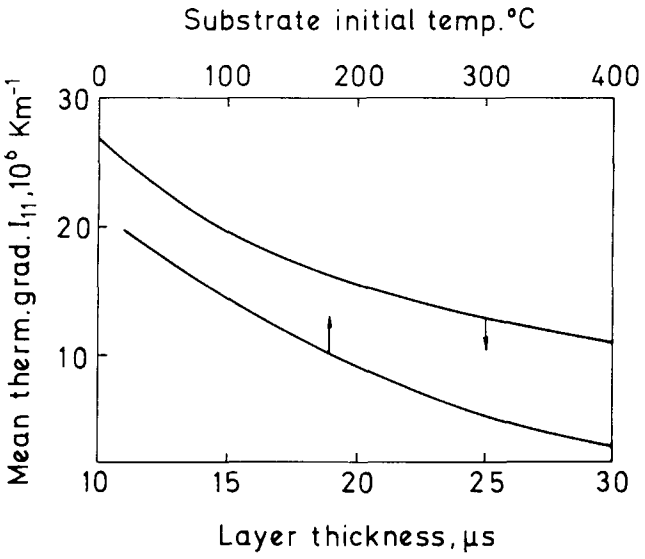

Fig. 9 Variation of mean thermal gradient I_{11} with respect to layer thickness and substrate initial temperature

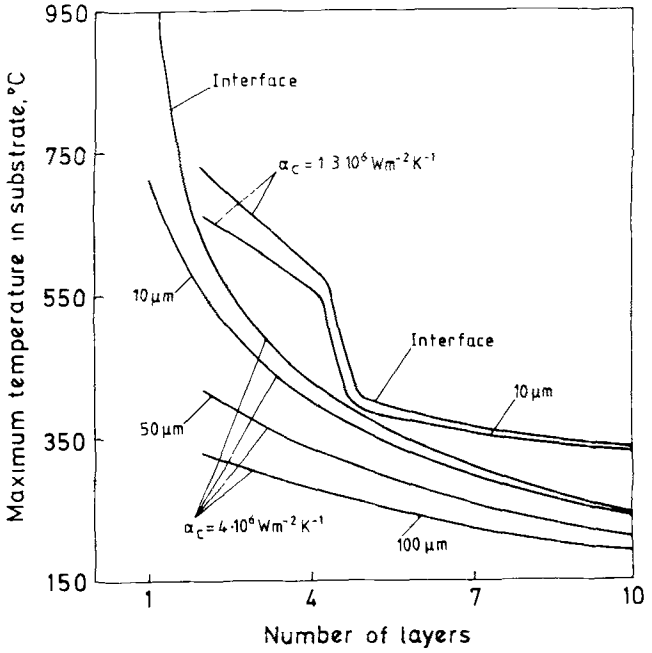

Fig. 10 Variation of maximum temperature at interface and different characteristic distances in substrate with respect to layer number

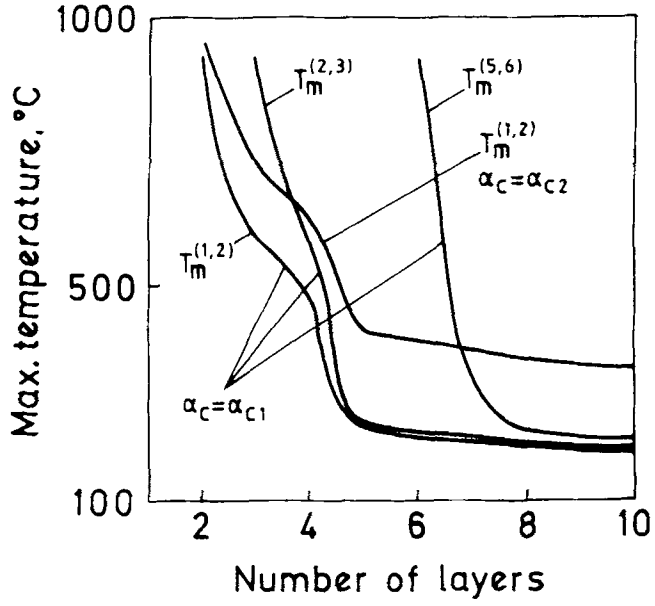

Fig. 11 Variation of maximum temperature at interfaces between different layers with respect to layer number

the thermal interaction between the substrate and the first coating layer.

The situation is different when the WC-Co coating is formed on the aluminum alloy substrate. Due to the thermophysical properties of this alloy, the subsequent coating layers markedly influence the heat transfer as well as the structure formation. The second layer has the most influence because the contact heat transfer coefficient between layers, α_{c2}, is higher than that of α_{c1} at the substrate-coating interface. Because of splashing by impinging droplets, forming of pores, etc., the coating layers are rougher than the original substrate and, therefore, have a higher α_c.

Calculations show that the time for full solidification of the second layer, τ_{sol}, is about 25% greater than that for the first layer because $\alpha_{c2} > \alpha_{c1}$. The second layer also influences the depths h_{Lm} and h_{Sm} of the isotherms of liquidus and solidus during the melting process in the substrate interfacial region. These parameters grow by about 10% of the values for heat transfer from the first layer. Thus, the heat transfer from the second layer leads to the remelting of the substrate interfacial region and its subsequent repeated solidification.

The influence of the third and subsequent layers is markedly smaller than that of the second layer. Figure 10 shows variation of maximum temperature at the substrate-coating interface and of characteristic distances in the substrate with layer number. These temperatures diminish with the increase of α_c and the layer number. Their variation is most pronounced at the interface and in the substrate interfacial region 10 μm from the interface. Figure 10 shows that substrate remelting at 10 μm ceases starting from the third layer and that the interface remelting ceases from the fourth layer.

The variation of the maximum temperature at the interfaces between the first and second layers ($T_m^{(1,2)}$), second and third layers ($T_m^{(2,3)}$), and fifth and sixth layers ($T_m^{(5,6)}$) with respect to the layer number is shown in Fig. 11. These temperatures decrease with increasing layer number and α_c. The $T_m^{(1,2)}$ temperature is changed mainly under the influence of four subsequent layers while $T_m^{(2,3)}$ and $T_m^{(5,6)}$ undergo their main variations under the influence of three subsequent layers. Thus, thermal interaction between the different coating layers is more substantial near the substrate-coating interface and decreases with increasing layer number.

The influence of this interaction on the structure formation is discussed in Ref 15.

4. Conclusions

- The full solidification time of the first coating layer increases with the layer thickness and initial substrate temperature. It varies nonuniformly with respect to the initial layer temperature.
- The first coating layer during solidification remains in the liquid or liquid-solid (mushy) state during much of its full solidification time: 60 to 80% in the liquid state and 20 to 40% in the mushy state, respectively.
- The mean thermal gradients in the layer with a solidifying phase, responsible for the development of thermal stresses, increase with layer thickness and initial temperature. They vary nonuniformly with initial substrate temperature.
- The minimal thermal stresses in the first coating layer (where they are higher than in the subsequent layers) are likely to occur when $T_{10} = 200$ °C and $T_{20} = 1495$ to 1500 °C. The maximal stresses seem to arise when $T_{10} = 300$ °C.
- The mean value of the solidifying alloy residence time in the mushy zone state varies nonuniformly with layer thickness, initial layer temperature, and initial substrate temperature.

- The best structural integrity in the coating layer is expected when $\delta = 10$ to 15 μm, $T_{10} = 20$ °C, and $T_{20} = 1510$ °C, and the worst is expected when $\delta = 20$ μm, $T_{10} = 300$ °C, and $T_{20} = 1550$ °C.
- The substrate interfacial region remains in the mushy state during much of its solidification. The zones of penetration of the liquidus and solidus isotherms into the substrate interfacial region during its melting increase with δ, T_{10}, and T_{20} and decrease with α_c. The maximum values of h_{Lm} and h_{Sm} increase when δ, T_{10}, and T_{20} grow. The difference between h_{Lm} and h_{Sm}, which determines the extent of the mushy zone region, increases with T_{10} and varies weakly with δ.
- The mean thermal gradient in the solidifying substrate interfacial region diminishes with increasing layer thickness and temperature and varies nonuniformly with respect to the initial substrate temperature. The minimal thermal stresses are expected when $T_{20} \approx 1510$ °C.
- The mean value of the residence time of the solidifying aluminum alloy in the mushy state grows with the initial layer temperature and varies nonuniformly with the layer thickness and initial substrate temperature. The optimal structure formed after solidification in the substrate interfacial region is expected when $\delta = 15$ to 22 μm and $T_{10} = 200$ °C.
- The time for full solidification of the second layer is about 25% greater than that for the first layer. Heat transfer from the second layer causes remelting of the substrate interfacial region and then its resolidification The influence of the third and the subsequent layers on the substrate-coating interfacial region is markedly smaller.
- The thermal interaction between different coating layers is more essential near the substrate-coating interface and decreases with increasing layer number.

Acknowledgments

The authors are grateful to the Generalitat de Catalunya (GC) for financial support received with project GRQ93-1017. V.V. Sobolev thanks GC for his visiting professor grant. J.A. Calero is also thankful to GC for the concession of a F.I. grant.

References

1. M.L. Thorpe and H.J. Richter, Pragmatic Analysis and Comparison of HVOF Processes, *J. Therm. Spray. Technol.*, Vol 1 (No. 2), 1992, p 161-170
2. D.W. Parker and G.L. Kutner, HVOF Moves into the Industrial Mainstream, *Adv. Mater. Process.*, No. 7, 1994, p 31-35
3. V.V. Sobolev, J.M. Guilemany, and J.A. Calero, Substrate-Coating Thermal Interaction During High Velocity Oxy-Fuel (HVOF) Spraying. Part 1. Heat Transfer Processes, *Mater. Sci. Technol.*, Vol 11, No. 8, 1995, p 810-819
4. V.V. Sobolev, J.M. Guilemany, and J.A. Calero, Substrate-Coating Thermal Interaction During High Velocity Oxy-Fuel (HVOF) Spraying. Part 2. Structure Formation, *Mater. Sci. Technol.*, Vol 11, No. 10, 1995
5. J.M. Guilemany, V.V. Sobolev, J. Nutting, Z. Dong, and J.A. Calero, Thermal Interaction Between WC-Co Coating and Steel Substrate in Process of HVOF Spraying, *Scr. Metall. Mater.*, Vol 31 (No. 7), 1994, p 915-920
6. V.V. Sobolev, J.M. Guilemany, J.R. Miguel, and J.A. Calero, Investigation of Coating Structure Development in Process of High Velocity Oxy-Fuel (HVOF) Spraying of WC-Ni Powder Particles, *Surf. Coat. Technol.*, in press, 1995
7. J. Nutting, J.M. Guilemany, and Z. Dong, The Substrate-Coating Interface Structure of a WC-Co HVOF Sprayed Coating onto Low Alloy Steel, *Mater. Sci. Technol.*, Vol 11, No. 9, 1995
8. V.V. Sobolev, J.M. Guilemany J.C. Garmier, and J.A. Calero, Modelling of Particle Movement and Thermal Behaviour During High Velocity Oxy-Fuel (HVOF) Spraying, *Surf. Coat. Technol.*, Vol 63, 1993, p 181-187
9. V.V. Sobolev, J.M. Guilemany, and J.A. Calero, Prediction of Behaviour of Powder Particles during High Velocity Oxy-Fuel (HVOF) Spraying. *J. Therm. Spray. Technol.*, Vol 4, No. 3, 1995, p 287-296
10. V.V. Sobolev and J.M. Guilemany, Investigation of Coating Porosity Formation During High Velocity Oxy-Fuel (HVOF) Spraying, *Mater. Lett.*, Vol 18, 1994, p 304-308
11. V.V. Sobolev and J.M. Guilemany, Analysis of Coating Gas Porosity Development During Thermal Spraying, *Surf. Coat. Technol.*, Vol 70, 1994, p 57-68
12. V.V. Sobolev and J.M. Guilemany, Flattening of Thermally Sprayed Particles, *Mater. Lett.*, Vol 22, 1995, p 209-213
13. D. Apelian, M. Paliwal, R.W. Smith, and W.F. Schilling, Melting and Solidification in Plasma Spray Deposition—Phenomenological Review, *Int. Met. Rev.*, Vol 28 (No. 5), 1983, p 271-284
14. L. Pawlowski and P. Fauchais, Thermal Transport Properties of Thermally Sprayed Coatings, *Int. Met. Rev.*, Vol 37 (No. 6), 1992, p 271-289
15. V.V. Sobolev, J.M. Guilemany, and J.A. Calero, Formation of Structure of WC-Co Coating on Aluminium Alloy Substrate During High Velocity Oxy-Fuel (HVOF) Spraying, in this issue, 1995
16. V.V. Sobolev and P.M. Trefilov, *Thermophysics of Metal Solidification During Continuous Casting*, Metallurgia, Moscow, 1988, p 68-75
17. A.J. Chapman, *Heat Transfer*, Macmillan, 1984, p 540
18. V.A. Wills and D.G. McCartney, Modelling of Dendritic Solidification Using Finite Element Method, Mater. Sci. Technol., Vol 8, 1992, p 144-122